Journal Pre-proof

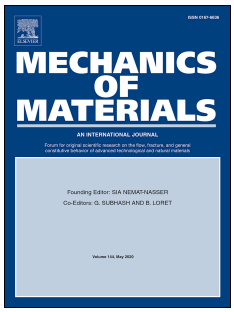

Analysis of the strain misfitbetween matrix and inclusions in a magnetically tunable composite

Federico Guillermo Bonifacich, Osvaldo Agustín Lambri, Fernando Daniel Lambri, Patricia Beatriz Bozzano, Vicente Recarte, Vicente Sánchez-Alarcos, José Ignacio Pérez-Landazábal

PII: S0167-6636(21)00269-6

DOI: https://doi.org/10.1016/j.mechmat.2021.104045

Reference: MECMAT 104045

To appear in: *Mechanics of Materials*

Received Date: 15 April 2021

Revised Date: 3 August 2021

Accepted Date: 27 August 2021

Please cite this article as: Bonifacich, F.G., Lambri, Osvaldo.Agustí., Lambri, F.D., Bozzano, P.B., Recarte, V., Sánchez-Alarcos, V., Pérez-Landazábal, José.Ignacio., Analysis of the strain misfitbetween matrix and inclusions in a magnetically tunable composite, *Mechanics of Materials* (2021), doi: https://doi.org/10.1016/j.mechmat.2021.104045.

Federico Guillermo Bonifacich: Conceptualization, Methodology, Investigation, Resources, Data curation, Writing-Original Draft, Writing-Review & Editing. **Osvaldo Agustín Lambri:** Conceptualization, Writing-Original Draft, Writing-Review & Editing, Visualization, Project administration. **Fernando Daniel Lambri:** Investigation, Resources, Data curation, Visualization. **Patricia Beatriz Bozzano**: Investigation, Resources, Data curation, Writing-Review & Editing Visualization. **V. Recarte:** Conceptualization, Writing-Review & Editing, Supervision, Visualization, Validation, Project administration.**V. Sánchez-Alarcos:** Methodology, Investigation, Resources, Data curation, Writing-Review & Editing. **J. I. Pérez-Landazábal:** Conceptualization, Writing-Review & Editing, Visualization, Project administration.

Analysis of the strain misfitbetween matrix and inclusions in a magnetically tunable composite

Federico Guillermo Bonifacich[1], Osvaldo Agustín Lambri[1], Fernando Daniel Lambri[1], Patricia Beatriz Bozzano[2], Vicente Recarte[3,4*], Vicente Sánchez-Alarcos[3,4], José Ignacio Pérez-Landazábal[3,4]

[1] CONICET-UNR. Laboratorio de Materiales, Escuela de Ingeniería Eléctrica, Centro de Tecnología e Investigación Eléctrica (CETIE), Facultad de Ciencias Exactas, Ingeniería y Agrimensura, Avda. Pellegrini 250, (2000) Rosario, Argentina

[2] Laboratorio de Microscopía Electrónica, Unidad de Actividad Materiales, Centro Atómico Constituyentes, Comisión Nacional de Energía Atómica e Instituto Sábato – Universidad Nacional de San Martín, Avda. Gral. Paz 1499, 1650 San Martín, Argentina

[3] Departamento de Ciencias, Universidad Pública de Navarra, Campus de Arrosadía, 31006 Pamplona, Spain

[4] Institute for Advanced Materials and Mathematics (INAMAT[2]), Universidad Pública de Navarra, Campus de Arrosadía, 31006 Pamplona, Spain

*Corresponding Author: Vicente Recarte

e-mail address: recarte@unavarra.es

Abstract

A magnetically tunable composite has been elaborated by embedding microparticles of a metamagnetic shape memory alloy on a photo curable resin. The strain misfit between the polymeric matrix and the inclusions has been analysed within Eshelby formalism. Results show the non-appearance of active microcracks at the interfaces where strains are induced by the martensitic transformation in the microparticles. Even though the martensitic transformation is well detected, the values of misfit β coefficient indicate that the matrix accommodates all the stresses induced by the inclusions. A stable surface interaction between particles and matrix is also confirmed during thermal cycles. It is also demonstrated that the damping capacity of the composites can be tuned by combining oscillating strain, fillers content and magnetic field. The proposed model could be applied to analyse the mechanical stability in polymer matrix composites in which fillers undergo a first order transition with volume change and associated deformation.

Keywords: Multifunctional composites; Polymer-matrix composites; Internal friction/damping; Stress transfer

1. Introduction

During last decade, Metamagnetic Shape Memory Alloys (MSMA) have focused a great interest and research activity coming from their potentiality as multifunctional materials. The multifunctional properties they show are linked to the occurrence of a first-order structural transition, the martensitic transformation (MT), between magnetically ordered phases. The interplay between structural transition and magnetic ordering opens the possibility of inducing the reverse MT by applying a magnetic field (Acet et al., 2011; Ito et al., 2007; Kainuma et al., 2006; Karaca et al., 2009; Koyama et al., 2006), giving rise to properties such as the magnetic actuation, the giant inverse magnetocaloric effect (MCE), giant magnetoresistance and magnetically tunable mechanical damping (Bonifacich et al., 2021; Bourgault et al., 2010; Gottschall et al., 2015; Krenke et al., 2007, 2005; Liu et al., 2012a; Planes et al., 2013, 2009; Sharma et al., 2006; Yu et al., 2006), that make these alloys very attractive for actuating and magnetic refrigeration applications. Nevertheless, one of the main drawbacks of these alloys is their poor mechanical properties, in particular the high brittleness. Composites made from polymeric matrix with metamagnetic shape memory powder alloys (where the polymer provides integrity and the alloy the functionality) have been recently proposed and developed to overcome the intrinsic brittleness of the bulk alloy (Feuchtwanger et al., 2005; Hosoda et al., 2004; Lahelin et al., 2009; Liu et al., 2012b, 2009).

Three-dimensional (3D) printing is an additive manufacturing technology that is becoming very popular because of its simplicity, relatively low cost, and unlimited creativity. This process enables the creation of complex three-dimensional objects, which cannot be cut, assembled or carved otherwise, having found numerous applications in a wide range of fields (Chen et al., 2019; Choi et al., 2015; Gul et al., 2018; Ngo et al.,

2018; Tan et al., 2017; Yan et al., 2018; Zhao et al., 2019). Among the different 3D printing techniques, photochemical approach has been proved to be very promising since well-defined structures can be created by photopolymerization of photocrosslinkable liquid resin under light irradiation, being also an economic and low environmental impact technique (Allen, 2010; Fouassier and Laleveé, 2012). Additive manufacturing of MSMA-polymer composites, which exhibit tunable (using an external magnetic field) properties, are referred to as 4D printed composites (Zhao et al., 2019). Recently, it has been shown that the damping capacity of a composite made with particles of a NiMnInCo MSMA into an UV-curing polymer can be tuned by applying low external magnetic fields (Bonifacich et al., 2021). This fact allows proposing this composite material to be used in the design of 4D printable devices for magneto-mechanical damping applications.

The strength of composites strongly depends on the optimal stress transfer between the fillers and the matrix. For well-bonded particles, the applied stress can be effectively transferred to the particles from the matrix and vice-versa (Hsueh, 1989); this clearly improves the strength (Nakamura et al., 1992; Pukanszky and VÖRÖS, 1993; Reynaud et al., 2001). On the other hand, the volume change and shear deformations associated with the MT (induced either by an external magnetic field or by changing temperature), generate stresses that should be properly transferred to the matrix. Monitoring internal stresses generated by the accommodation between matrix and MSMA inclusions gives information about the stability of the interphase. In this work, a commercial photo curable Bis-GMA resin has been used to produce composites with microparticles of a $Ni_{45}Mn_{36.7}In_{13.3}Co_5$MSMA. The results show the non-appearance of active microcracks at the interface during the MT. The strain misfit between matrix and fillers exhibits an overall enhancement with temperature and confirms that the matrix accommodates all the stresses induced by the inclusions. Besides, a stable surface

interaction between the particles and the matrix during thermal cycles has been confirmed. The possibility of tuning the damping capacity of composites by combining oscillating strain, the fillers content and magnetic field intensity is highlighted.

2. Materials and methods

Bulk $Ni_{45}Mn_{36.7}In_{13.3}Co_5$ MSMA were hand milled, sieved and annealed at 423 K. Particles smaller than 63μm were used as fillers to prepare polymeric composites. The polymeric matrix used was a commercial photo curable bisphenol A-glycidyl methacrylate (Bis-GMA) resin produced by Schmidt (Composite flow). The polymer was cured using an exposure to UV light (600 $mWcm^{-2}$, 410 nm) at room temperature (RT) during 80 s. Composites with 1.1%, 2.6%, 6.2% and 12.8%, volume fractions of fillers were prepared and will be referred hereafter as C011, C026, C062 and C128, respectively (see (Bonifacich et al., 2021) for more details).

The MT temperatures were determined from magnetization measured in a SQUID magnetometer (QD MPMS XL-7). Scanning electron microscopy (SEM) images of the composite samples were performed under vacuum in a FEI Quanta 200 scanning electron microscope operated at 20 kV. Dynamic Mechanical Analysis (DMA) measurements, loss tangent (tan(ϕ), damping or internal friction), Q^{-1}, and dynamic shear modulus, G', were carried out as a function of temperature under Argon at atmospheric pressure. The samples for DMA were parallelepiped bars with dimensionsof 1 x 1 x 20 mm^3. The maximum shear strain at the surface of the sample was $2 \cdot 10^{-4}$. Measurements were performed during heating and cooling at 1K min^{-1} in the 220-400K temperature range, at frequencies close to 5 Hz. Two successive heating and cooling runs were performed on each kind of samples; where there were not hold time neither at the minimum nor at the

maximum temperatures. Nonetheless, for the sample with the highest particles content, ten thermal cycles were performed to explore the stability of the composite.

Amplitude dependent damping (ADD), i.e. damping as a function of the maximum strain on the sample, ε_0, was calculated using eq. (1) (Lambri, 2000; Molinas et al., 1994; Zelada-Lambri et al., 2006):

$$Q^{-1}(\varepsilon_0) = -\frac{1}{\pi}\frac{\mathrm{d}(\ln(A_n))}{\mathrm{dn}} \quad (1)$$

where: A_n is the area of the nth decaying oscillation and n is the period number. The explored values of ε_0 range in the 5-20 $\cdot 10^{-5}$ interval. Therefore, the Q^{-1} (T, ε_0) was determined in the analysed temperature and amplitude ranges.

The decay of the torsional oscillations was measured at nearly constant temperature (T ± 0.5 K). Decaying areas as a function of n were fitted to a polynomial (up to 3rd order) in order to determine the damping as a function of the maximum strain (ε_0). Polynomials of degree higher than 1 indicate that Q^{-1} is a function of ε_0, leading to ADD effects (Lambri, 2000; Molinas et al., 1994; Zelada-Lambri et al., 2006). The strength of ADD can be quantified using the S coefficient (Lambri, 2000; Molinas et al., 1994; Zelada-Lambri et al., 2006):

$$S = \frac{\Delta Q^{-1}}{\Delta \varepsilon_0} \quad (2)$$

where ΔQ^{-1} is the damping change corresponding to the full amplitude change $\Delta\varepsilon_0$ measured in the whole oscillating strain range.

3. Results and Discussion

The martensitic transformation in the fillers and the magnetic response of the composite have been determined from magnetization measurements. Figure 1 shows the

temperature dependence of magnetization under 100 Oe applied magnetic field for the C128 composite. The occurrence of the MTin the microparticles is evidenced by the large magnetization jump taking place around 300 K, which shows the characteristic thermal hysteresis. Another magnetization jump related to the ferro-para magnetic transition takes place at the Curie temperature of 380 K. As shown in the inset, the application of a high magnetic field causes a large shift of the MT to lower temperatures. In particular, the temperature at which the transformation from martensite to austenite begins on heating, A_S (austenite start), decreases from 280 K to 240 K under 60 kOe applied field, thus resulting in a magnetically induced structural phase transition. The characteristic temperatures obtained from the SQUID measurements shown in Figure 1 were determined as the intersection of the tangent lines of the curve on either side of the change in the slope of the magnetization curve. Taking into account the different mechanical properties of the austenite and martensite phases, this allows the magnetically tuning of the damping capacity of a composite (Bonifacich et al., 2021).

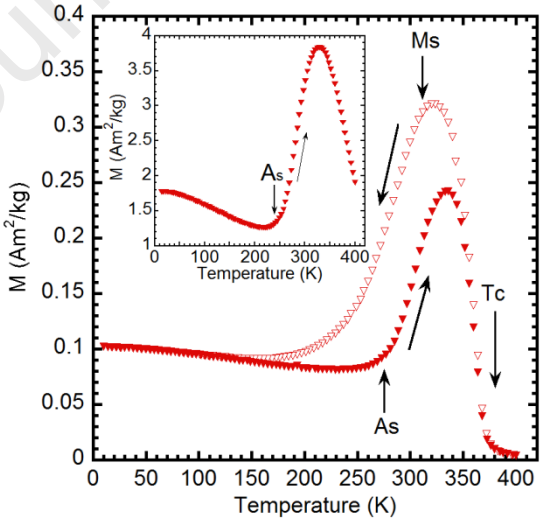

Fig. 1 Temperature dependence of magnetization under 100 Oe applied magnetic field for the C128 composite. Inset: Heating M(T) curve under 60 kOe.

3.1.Amplitude Dependent Damping (ADD)

The MT involves non-linear mechanisms leading to non-linear damping, i.e. amplitude dependent damping (ADD) (Cahn et al. 1994; Schaller et al., 2001). In fact, the movement of the martensite variants in martensitic phase and the movement of martensite/austenite interface during the MT lead to ADD during the DMA measurements (Bonifacich et al., 2016; Lambri et al., 2015; Pérez-Landazábal et al., 2015; Van Humbeeck, 1985).

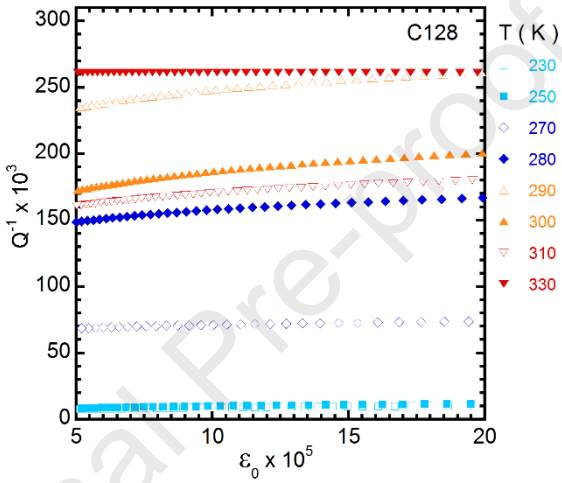

Fig. 2 Q^{-1} (T=*constant*, ε_0) vs. the maximum strain (ε_0) for the C128 composite in the 220-330 K temperature range.

Figure 2 shows the Q^{-1} (ε_0) vs.the maximum strain (ε_0) for the C128 composite in the 220-330 K temperature range (not all curves are shown for clarity but its description is similar). Except the measurement at 330 K that shows a constant value, all curves show increasing values indicating an ADD. In composite materials, the study of damping as a function of strain is an important tool to determine the appearance of microcracks at the interfaces between inclusion and matrix (Lambri, 2000; Lambri et al., 2012; Lazan, 1968; Mocellini et al., 2017). The appearance of mechanically active interfaces in composite materials, e.g. by microcracks lying at the interface, implies that Q^{-1} describes a peaked shaped curve as function of ε_0. The presence of a maximum in the ADD curves can be

easily understood considering the definition of damping, i.e. $Q^{-1} = \Delta W / W$, where ΔW is the irreversible energy lossper cycle and W is the stored elastic energy. The appearance of de-bonding at the interfaces, or active microcracks, leads to values of ΔW which will be nearly constant independently of the applied strain, but W will vary as the oscillating strain increases (Lambri, 2000; Lambri et al., 2012; Lazan, 1968; Mocellini et al., 2017). In the present case, Q^{-1} vs ε_0 curves show a monotonous increase as a function of the maximum oscillating strain, ε_0. Thus, within the oscillating strain range used, a maximum in the Q^{-1} vs ε_0 does not to occur. Therefore, the Q^{-1} vs ε_0 plots in Figure 2 confirm the non-appearance of active microcracks at the interface between the inclusions and matrix where induced strains appear as a consequence of the MT. This point is relevant from the point of view of the mechanical properties in composite materials (Bonifacich et al., 2021; Kato et al., 1996; Lee et al., 1980; Liu et al., 2012b; Mocellini et al., 2017; Mori and Wakashima, 1990).

The non-appearance of microcracks was also confirmed by SEM studies. Figure 3 shows SEM images of MSMA particles embedded in the polymer matrix for a C128 sample, which reflects the general appearance of the particles in the different regions of the composite. The SEM images show a sharp interface with no cracks on the interfaces between MSMA particles and the polymer matrix at least within the resolution of the equipment.

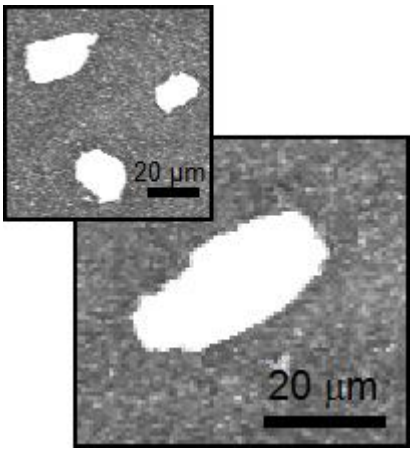

Fig. 3 SEM micrograph of a C128 composite sample.

Figure 4 shows Q^{-1} (T) as a function of temperature for the extreme values of ε_0 ($5 \cdot 10^{-5}$ and $20 \cdot 10^{-5}$) for samples C011 (a), C062 (b) and C128 (c). Q^{-1} was also measured under an external magnetic field (HDC) of 100 kA/m for C062 (b) and C128 (c) samples. Samples with a lower filler content hardly show detectable differences with the magnetic field. The parallel evolution of the dynamic shear modulus (G') is also shown in Figure 4.d together with the G´ temperature dependence of the polymeric matrix. The damping peak between 250 K and 320 K (b-c) and its G´ defect (d) was recently related to the MT process (Bonifacich et al., 2021). In fact, the damping peak was linked to the thermally induced mobility of the austenite-martensite interfaces that occurs inside the fillers (Bonifacich et al., 2021; Pérez-Sáez et al., 1998; R. Schaller et al., 2001). The thermal hysteresis found in both Q^{-1} and G' curves increase with the volume fraction of fillers. Although the MT-peak is not clear in the C011 composite due to the low volume fraction of fillers, the hysteresis is observed in both, the damping and the shear modulus curves. Once the fillers undergo the complete phase transformation, i.e. MSMA-fillers are full martensite or full austenite, the difference between heating and cooling disappears (Bonifacich et al., 2021). No difference appears in DMA studies during two consecutive

thermal cycles performed for all composite samples. Moreover, ten thermal cycles were carried out only for the sample C128, where no differences bwtween curves were found.

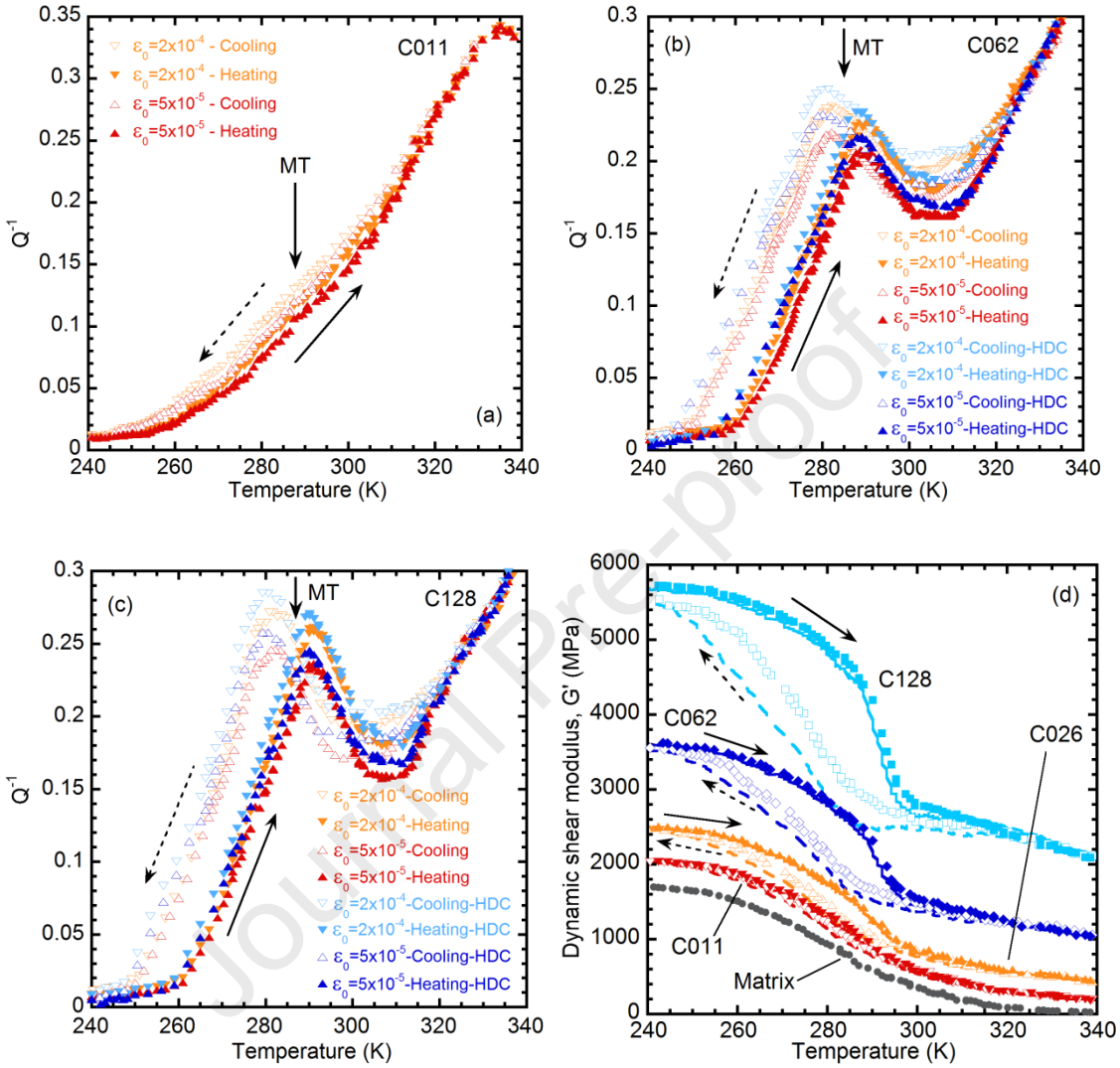

Fig. 4 Q^{-1} (T, ε_0=constant) as a function of temperature for the extreme values of ε_0 ($5 \cdot 10^{-5}$ and $20 \cdot 10^{-5}$) for samples C011 (a), C062 (b) and C128 (c). Q^{-1} was also measured under an external magnetic field (HDC) of 100 kA/m for C062 (b) and C128 (c) samples. Full symbols: heating run. Empty symbols: cooling run. Arrows indicate the increase and the decrease in temperature. (d) Temperature dependence of the dynamic shear modulus, G' (also for the polymeric matrix, grey circles), measured under magnetic field during the heating (full lines) and cooling (broken lines).

Damping increases with the strain amplitude ε_0 only in the 240 K - 310 K temperature range. Outside this range, the inclusions of $Ni_{45}Mn_{36.7}In_{13.3}Co_5$ MSMA are entirely in martensitic or austenite. Besides, the matrix (without fillers) does not reveal

any amplitude dependent effect. So, the non-linear effects found are promoted by the existence of martensite/martensite and martensite/austenite interfaces present during the MT in the MSMA-fillers) (Bonifacich et al., 2016; Cahn et al. 1994; Kartasheva et al., 2017; Lambri et al., 2015; Pérez-Landazábal et al., 2015; Salas et al., 2012; Schaller et al., 2001; Van Humbeeck, 1985). In fact, the movement of the austenite/martensite interfaces is strain amplitude dependent (Schaller et al., 2001). ADD in the MT-peak is related to the dynamics of the martensitic phase transformation and consequently, the intrinsic, transient and phase transformation (mainly dependent on the austenite/martensite movement) damping contributions must be taken into account (Pérez-Sáez, 1998). The ADD degree is higher for C128 than for C011 due to its higher volume fraction of inclusions. Nevertheless, non-linear effects have not been observed in the usually less sensitive dynamic shear modulus $G´$ (Lazan, 1968; Mocellini et al., 2017). In all cases, the applied magnetic field (HDC) increases the MT-peak height. Therefore, a combined increase of the strain amplitude of the solicitations, the fillers content and the applied magnetic field leads to an increase in the MT-peak height (up to around 5 times) and then an improvement in the capability of absorbing mechanical vibrations can be obtained. For instance, the damping values for C128 sample, increase about a 3% under magnetic field and about an 11% when the maximum oscillating strain increases from $5 \cdot 10^{-5}$ to $20 \cdot 10^{-5}$. Combining both effects, an increase of around 16% can be observed. Therefore, the capacity of tuning of these composite samples by combining oscillating strain, the fillers content and magnetic field intensity should be highlighted.

The S coefficient (eq. 2) allows to make more evident the ADD effect (Lambri, 2000; Molinas et al., 1994; Zelada-Lambri et al., 2006). Figure 5 shows the temperature dependence of the S coefficient in the 220 K- 340 K range (for clarity, the curves were vertically shifted). The S curves describe a hysteretic broad peak in the MT temperature

range. In addition, the S values increases with the increase in filler concentration. In fact, the S change associated to the MT in the C128 sample is around five times higher than in the C011 sample. Therefore, the S evolution should be correlated to the damping mechanisms linked to the MT which are strain dependent (Bonifacich et al., 2016; Cahn et al. 1994; Pérez-Landazábal et al., 2015; Schaller et al., 2001). Above the MT temperature range, the S values decreases but in all cases a superimposed second stage appears more evidently for high filler concentration. This second stage could be related to the interaction between point defects and dislocations, or to the interaction between dislocations and magnetic domains in the ferromagnetic austenite (Bonifacich et al., 2016; Bonifacich et al., 2017; Cahn et al. 1994; Lambri et al., 2021; Pérez-Landazábal et al., 2015; Schaller et al., 2001). Further studies (beyond the aim of this work) should be needed to clarify this point.

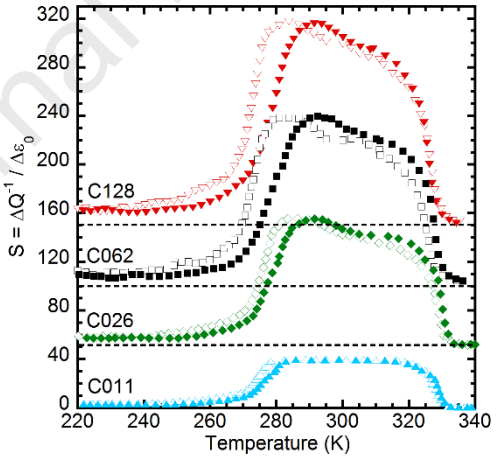

Fig. 5 Temperature dependence of the S coefficient in the 220 K- 340 K range (for clarity, the curves were vertically shifted) during heating (full symbols) and cooling (empty symbols).

3.2.Strain misfit and elastic energy transference

The internal stresses generated by the accommodation misfit between matrix and inclusion-particles in a composite material have been analyzed within the Eshelby

approach (Eshelby and Peierls, 1957; Mori and Tanaka, 1973; Mura, 1987), through a model originally developed for describing the elastic misfit in two-phase polymer (Mocellini et al., 2009). The model considers an elastic, infinite, homogeneous and isotropic matrix (polymer Bis-GMA) and hollows inner regions (holes), where larger inclusions are putted ($Ni_{45}Mn_{36.7}In_{13.3}Co_5$ MSMA-particles). From the mechanical equilibium condition at the boundary between the matrix and inclusion elements, considering a pure Reuss aproximation, a misfitting coefficient, β, as a function of the Young moduli, E, and inclusions and matrix volume fractions was obtained (Mocellini et al., 2009),

$$\beta = \frac{1}{1+\left(\frac{E_m}{E_i}\right)\cdot\left(\frac{fr_i}{fr_m}\right)} \tag{3}$$

where fr_i, fr_m, E_i and E_m are the volume fraction and the elastic modulus of the inclusions and matrix, respectively. The misfit coefficient β relates the inclusion strain caused by the matrix (or vice versa). Values of β trend to 1 indicate that the inclusion strongly deforms the composite matrix. Contrastingly, a decrease in β values from 1 towards smaller values indicates that the inclusion is suffering a stressing from the matrix. See for more details (Mocellini et al., 2009).

On the other side, inclusion from its initial compressed state to the final equilibrium state gives rise to a transference of elastic energy to the matrix. The ratio between the density of elastic energy transferred to the matrix (w_m) and the total available density of elastic energy (w_T) can be described as (Lambri et al., 2011)

$$\frac{w_m}{w_T} = \frac{E_m}{E_i}\beta^2\left(\frac{fr_i}{1-fr_i}\right) \tag{4}$$

Nevertheless, in several cases, the Reuss approximation used to get eqs. (3) and (4) is not entirely appropriated (Mura, 1987). So, a more general relationship between the actual modulus of the composite (E) and the moduli using the Voigt (E_V) and Reuss (E_R) approximations has been proposed (Bonifacich et al., 2021).

$$E = pE_V + (1-p)E_R \tag{5}$$

where p is the weighting factor such that $0 < p \leq 1$. In the present case, a $p = 0.25$ value was determined (Bonifacich et al., 2021). Then, the ratio of applied external stress transmitted uniformly trough the composite is (1 - p). Consequently,

$$\sigma_i(1-p) = \sigma_m \tag{6}$$

Where σ_i and σ_m are the stress in the inclusion and in the matrix, respectively. Thus, the β coefficient, for a non-pure Reuss condition, takes the form

$$\beta = \frac{1}{1+\left(\frac{E_m}{E_i(1-p)}\right)\cdot\left(\frac{fr_i}{fr_m}\right)} \tag{7}$$

In the same way, the ratio between the density of elastic energy transferred to the matrix and the available density of elastic energy can be modified as

$$\frac{w_m}{w_T} = \frac{E_m}{E_i(1-p)}\beta^2\left(\frac{fr_i}{1-fr_i}\right) \tag{8}$$

The evolution of the β coefficient on heating and cooling are shown in Figure 6.a. In order to determine the β coefficient (see eq. 7), the volume fraction of inclusions, the modulus of the matrix (Figure 4.d) and the modulus of the MSMA particles have been taken from (Bonifacich et al., 2021) (see inset in Figure 6).The β coefficient exhibits an overall increase with temperature, mainly controlled by the softening of the polymeric matrix (see grey circles in Figure 4.d). As the temperature increases, the matrix can accommodate better the internal stresses induced by the MSMA particles, since $\beta \rightarrow 1$.

The opposite occurs on cooling; some strain is induced over the MSMA particles, i.e. the internal stresses on the MSMA particles increase. Besides, the β coefficient decreases as the volume fraction of MSMA inclusions increases due to the lower capability of the matrix to accommodate stresses (Lambri et al., 2014). Therefore, the particles will suffer more misfit deformation as the volume fraction of particles increases.

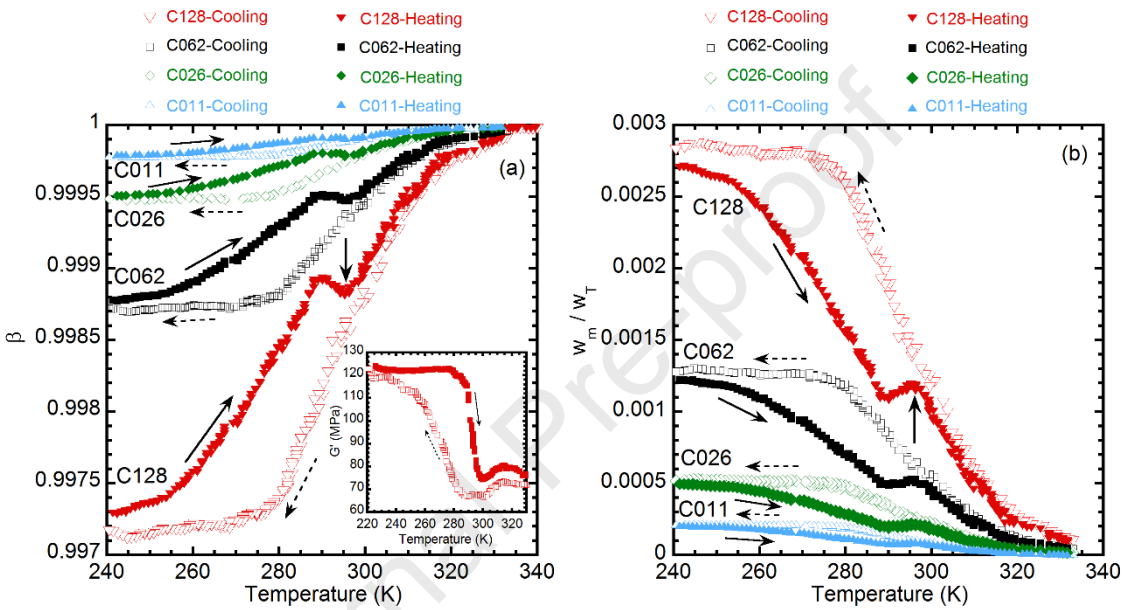

Fig. 6 Temperature dependence of the β coefficient (a) and (w_m/ w_T) (b) during heating (full symbols) and cooling (empty symbols).

The MT induces an inverted peak superimposed to the whole trend of β coefficient measured during heating (marked by an arrow for C128); the higher is the volume fraction of MSMA particles, the deeper the peak is.The inverted peak reveals that the particles are being deformed by the matrix in order to accommodate the strain misfit.This agrees with the softening of MSMA particles around the MT (see inset). The thermal hysteresis clearly increases with the volume fraction of MSMA particle, though the effect on cooling is quite less marked.

In order to understand the physical processes controlling the shape of β parameter on cooling, the temperature dependence of the ratio w_m/w_T (eq. 8) has been analysed. As

shown in Figure 6.b, the ratio w_m/w_T decreases with temperature since w_m decreases as a consequence of the reduction of the elastic modulus of the polymer (w_m is proportional to the elastic modulus). In addition, w_m/w_T increases with the volume fraction of MSMA particles due to the increase in available energy to be transferred to the matrix (w_T) when the amount of particles increases. Again, during heating, a superimposed peak associated to the MT appears. The peak height increases with the volume fraction of particles. This peak is related to the decrease of w_T associated to the modulus softening of the MSMA particles in the MT. Moreover, the peak in w_m/w_T can be observed even in the C011 sample, indicating that the ratio w_m/w_T is more sensitive to the MT than the misfit coefficient. On cooling, in turn, the modulus values are lower than on heating within the temperature range of the MT (see inset in Figure 6.a), which results in a lower availability of the energy to be transferred to the matrix. Therefore, the temperature dependence of β and w_m/w_T ratio on cooling is the result of the effect of the hysteretic behaviour in the modulus on the competence between the modulus of the matrix and the MSMA inclusions. Finally, it is worth mentioning that the behaviour of both β and w_m/w_T parameters does not evolve during subsequent thermal cycles, pointing out a large stability of the surface interaction between the particles and the matrix, in agreement with the above-mentioned non-appearance of microcracks.

4. Conclusions

The strain misfit between the polymeric matrix and the metallic inclusions has been analysed within Eshelby formalism. Results show the non-appearance of active microcracks at the interface where induced strains appear as a consequence of the martensitic transformation in the microparticles. On the other hand, even though the

martensitic transformation is well detected, the misfit coefficient exhibits values close to 1, indicating that the matrix accommodates all the stresses induced by the inclusions. A stable surface interaction between the particles and the matrix is also confirmed during thermal cycles. It is also demonstrated that the tuning capacity of the elaborated composites can be modified by combining oscillating strain, the fillers content and the magnetic field intensity. The proposed model could be applied to analyse the stability and stress accommodation in any polymer matrix composites in which the filler material undergoes a first order phase transitions with volume changes and an associated deformation.

Acknowledgements

This work has been partially supported by PID-UNR ING 575 and ING 612 (2018–2021), Agencia de Investigación de la Provincia de Santa Fe (Cod IO-2017-00138, Res. 177/18), Project RTI2018-094683-B-C54 (MCIU/AEI/FEDER,UE), Project PC017-018 AMELEC (Navarra Government) and the Cooperation Agreement between the Universidad Nacional de Rosario and the Universidad Pública de Navarra, Res. C.S. 3247/2015.

References

Acet, M., Mañosa, L., Planes, A., 2011. Chapter Four - Magnetic-Field-Induced Effects in Martensitic Heusler-Based Magnetic Shape Memory Alloys, in: Buschow, K.H.J. (Ed.), Handbook of Magnetic Materials. Elsevier, pp. 231–289. https://doi.org/https://doi.org/10.1016/B978-0-444-53780-5.00004-1

Allen, N.S., 2010. Photochemistry and photophysics of polymer materials. John Wiley & Sons Inc, New York.

Bonifacich, F.G., Lambri, O.A., Pérez-Landazábal, J.I., Gargicevich, D., Recarte, V., Sánchez-Alarcos, V., 2016. Mobility of Twin Boundaries in Fe-Pd-Based Ferromagnetic Shape Memory Alloys. Mater. Trans. 57, 1837–1844.

https://doi.org/10.2320/matertrans.M2016243

Bonifacich, F.G., Lambri, O.A., Recarte, V., Sánchez-Alarcos, V., Pérez-Landazábal, J.I., 2021. Magnetically tunable damping in composites for 4D printing. Compos. Sci. Technol. 201, 108538. https://doi.org/10.1016/j.compscitech.2020.108538

Bonifacich, F.G., Pérez-Landazábal, J.I., Lambri, O.A., Bozzano, P.B., Sánchez-Alarcos, V., García, J.A., Zelada, G.I., Recarte, V., Cuello, G.J., 2017. Influence of thermal treatments on the mechanical properties and the martensitic transformation in Fe-Pd-Mn ferromagnetic shape memory alloy. Mater. Sci. Eng. A 683, 164–171. https://doi.org/10.1016/j.msea.2016.12.012

Bourgault, D., Tillier, J., Courtois, P., Maillard, D., Chaud, X., 2010. Large inverse magnetocaloric effect in Ni45Co5Mn37.5In12.5 single crystal above 300 K. Appl. Phys. Lett. 96, 132501. https://doi.org/10.1063/1.3372633

Cahn, R.W., Haasen, P., Kramer, E. J., 1994. Materials science and technology A comprehensive treatment. Volume 2B: Characterization of Materials (Part II), in: Lifshin, E. (Ed.) VCH, Weinheim. https://doi.org/10.1002/crat.2170290603

Chen, Z., Li, Z., Li, J., Liu, Chengbo, Lao, C., Fu, Y., Liu, Changyong, Li, Y., Wang, P., He, Y., 2019. 3D printing of ceramics: A review. J. Eur. Ceram. Soc. 39, 661–687. https://doi.org/10.1016/j.jeurceramsoc.2018.11.013

Choi, J., Kwon, O.-C., Jo, W., Lee, H.J., Moon, M.-W., 2015. 4D Printing Technology: A Review. 3D Print. Addit. Manuf. 2, 159–167. https://doi.org/10.1089/3dp.2015.0039

Eshelby, J.D., Peierls, R.E., 1957. The determination of the elastic field of an ellipsoidal inclusion, and related problems. Proc. R. Soc. London. Ser. A. Math. Phys. Sci. 241, 376–396. https://doi.org/10.1098/rspa.1957.0133

Feuchtwanger, J., Richard, M.L., Tang, Y.J., Berkowitz, A.E., O'Handley, R.C., Allen, S.M., 2005. Large energy absorption in Ni–Mn–Ga/polymer composites. J. Appl. Phys. 97, 10M319. https://doi.org/10.1063/1.1857653

Fouassier, J.P., Laleveé, J., 2012. Photoinitiators for Polymer Synthesis-Scope, Reactivity, and Efficiency. Wiley-VCH Verlag GmbH & Co KGaA, Weinheim.

Gottschall, T., Skokov, K.P., Frincu, B., Gutfleisch, O., 2015. Large reversible magnetocaloric effect in Ni-Mn-In-Co. Appl. Phys. Lett. 106, 21901. https://doi.org/10.1063/1.4905371

Gul, J.Z., Sajid, M., Rehman, M.M., Siddiqui, G.U., Shah, I., Kim, K.-H., Lee, J.-W., Choi, K.H., 2018. 3D printing for soft robotics – a review. Sci. Technol. Adv. Mater. 19, 243–262. https://doi.org/10.1080/14686996.2018.1431862

Hosoda, H., Takeuchi, S., Inamura, T., Wakashima, K., 2004. Material design and shape memory properties of smart composites composed of polymer and ferromagnetic shape memory alloy particles. Sci. Technol. Adv. Mater. 5, 503–509.

https://doi.org/10.1016/j.stam.2004.02.009

Hsueh, C.H., 1989. Effects of Aspect Ratios of Ellipsoidal Inclusions on Elastic Stress Transfer of Ceramic Composites. J. Am. Ceram. Soc. 72, 344–347. https://doi.org/10.1111/j.1151-2916.1989.tb06132.x

Ito, W., Imano, Y., Kainuma, R., Sutou, Y., Oikawa, K., Ishida, K., 2007. Martensitic and Magnetic Transformation Behaviors in Heusler-Type NiMnIn and NiCoMnIn Metamagnetic Shape Memory Alloys. Metall. Mater. Trans. A 38, 759–766. https://doi.org/10.1007/s11661-007-9094-9

Kainuma, R., Imano, Y., Ito, W., Sutou, Y., Morito, H., Okamoto, S., Kitakami, O., Oikawa, K., Fujita, A., Kanomata, T., Ishida, K., 2006. Magnetic-field-induced shape recovery by reverse phase transformation. Nature 439, 957–960. https://doi.org/10.1038/nature04493

Karaca, H.E., Karaman, I., Basaran, B., Ren, Y., Chumlyakov, Y.I., Maier, H.J., 2009. Magnetic Field-Induced Phase Transformation in NiMnCoIn Magnetic Shape-Memory Alloys—A New Actuation Mechanism with Large Work Output. Adv. Funct. Mater. 19, 983–998. https://doi.org/10.1002/adfm.200801322

Kartasheva, N., Liubimova, Y., Salas, D., Kustov, S., 2017. Dynamic magnetic characteristics during martensitic transformations in NiMnInCo metamagnetic shape memory alloy. Mater. Today Proc. 4, 4768–4772. https://doi.org/10.1016/j.matpr.2017.04.068

Kato, M., Fujii, T., Onaka, S., 1996. Elastic strain energies of sphere, plate and needle inclusions. Mater. Sci. Eng. A 211, 95–103. https://doi.org/10.1016/0921-5093(95)10091-1

Koyama, K., Watanabe, K., Kanomata, T., Kainuma, R., Oikawa, K., Ishida, K., 2006. Observation of field-induced reverse transformation in ferromagnetic shape memory alloy Ni50Mn36Sn14. Appl. Phys. Lett. 88, 132505. https://doi.org/10.1063/1.2189916

Krenke, T., Duman, E., Acet, M., Wassermann, E.F., Moya, X., Mañosa, L., Planes, A., 2005. Inverse magnetocaloric effect in ferromagnetic Ni-Mn-Sn alloys. Nat. Mater. 4, 450–4. https://doi.org/10.1038/nmat1395

Krenke, T., Duman, E., Acet, M., Wassermann, E.F., Moya, X., Mañosa, L., Planes, A., Suard, E., Ouladdiaf, B., 2007. Magnetic superelasticity and inverse magnetocaloric effect in Ni-Mn-In. Phys. Rev. B 75, 1–6. https://doi.org/10.1103/PhysRevB.75.104414

Lahelin, M., Aaltio, I., Heczko, O., Söderberg, O., Ge, Y., Löfgren, B., Hannula, S.P., Seppälä, J., 2009. DMA testing of Ni–Mn–Ga/polymer composites. Compos. Part A Appl. Sci. Manuf. 40, 125–129. https://doi.org/10.1016/j.compositesa.2008.10.011

Lambri, O.A., 2000. A Review on the Problem of Measuring Non-Linear Damping and the Obtainment of Intrinsic Damping, in: Martinez-Mardones, J., Walgraef, D., Wörner, C.H. (Eds.), Materials Instabilities. World Scientific Publishing, New York, pp. 249–280. https://doi.org/10.1142/9789812793317_0005

Lambri, O.A., Gargicevich, D., Tarditti, F., Bonifacich, F.G., Riehemann, W., Anhalt, M., Weidenfeller, B., 2012. Magnetic Field Dependent Damping of Magnetic Particle Filled Polypropylene. Solid State Phenom. 184, 449–454. https://doi.org/10.4028/www.scientific.net/SSP.184.449

Lambri, O.A., Mocellini, R.R., Tarditti, F., Bonifacich, F.G., Gargicevich, D., Zelada, G.I., Boschetti, C.E., 2014. Internal stresses in the electrostriction phenomenon viewed through dynamic mechanical analysis studies conducted under electric field. IEEE Trans. Dielectr. Electr. Insul. 21, 2070–2080. https://doi.org/10.1109/TDEI.2014.004365

Lambri, O.A., Pérez-Landazábal, J.I., Gargicevich, D., Recarte, V., Bonifacich, F.G., Cuello, G.J., Sánchez-Alarcos, V., 2015. Order evolution in iron-based alloys viewed through amplitude dependent damping studies. Mater. Trans. 56, 182–186. https://doi.org/10.2320/matertrans.M2014397

Lambri, O.A., Plazaola, F., Axpe, E., Mocellini, R.R., Zelada-Lambri, G.I., García, J.A., Matteo, C.L., Sorichetti, P.A., 2011. Modification of the mesoscopic structure in neutron irradiated EPDM viewed through positron annihilation spectroscopy and dynamic mechanical analysis. Nucl. Instruments Methods Phys. Res. Sect. B Beam Interact. with Mater. Atoms 269, 336–344. https://doi.org/10.1016/j.nimb.2010.11.095

Lambri, O.A., Weidenfeller, B., Bonifacich, F.G., Pérez-Landazábal, J.I., Cuello, G.J., Weidenfeller, L., Recarte, V., Zelada, G.I., Riehemann, W., 2021. Magnetic behavior in commercial iron-silicon alloys controlled by the dislocation dynamics at temperatures below 420 K. J. Alloys Compd. 856, 157934. https://doi.org/10.1016/j.jallcom.2020.157934

Lazan, B.J., 1968. Damping of materials and members in structural mechanics. Pergamon, London.

Lee, J.K., Earmme, Y.Y., Aaronson, H.I., Russell, K.C., 1980. Plastic relaxation of the transformation strain energy of a misfitting spherical precipitate: Ideal plastic behavior. Metall. Trans. A 11, 1837–1847. https://doi.org/10.1007/BF02655099

Liu, J., Gottschall, T., Skokov, K.P., Moore, J.D., Gutfleisch, O., 2012a. Giant magnetocaloric effect driven by structural transitions. Nat. Mater. 11, 620–626. https://doi.org/10.1038/nmat3334

Liu, J., Scheerbaum, N., Kauffmann-Weiss, S., Gutfleisch, O., 2012b. NiMn-Based Alloys and Composites for Magnetically Controlled Dampers and Actuators. Adv. Eng. Mater. 14, 653–667. https://doi.org/10.1002/adem.201200038

Liu, J., Scheerbaum, N., Weiß, S., Gutfleisch, O., 2009. Ni–Mn–In–Co single-crystalline particles for magnetic shape memory composites. Appl. Phys. Lett. 95, 152503. https://doi.org/10.1063/1.3249585

Mocellini, R.R., Lambri, O.A., Gargicevich, D., Bonifacich, F.G., Weidenfeller, B., Anhalt, M.,

Riehemann, W., 2017. Magnetic memory effect in magnetite charged polypropylene composite. Compos. Interfaces 24, 611–633. https://doi.org/10.1080/09276440.2017.1250548

Mocellini, R.R., Lambri, O.A., Matteo, C.L., García, J.A., Zelada-Lambri, G.I., Sorichetti, P.A., Plazaola, F., Rodríguez-Garraza, A., Sánchez, F.A., 2009. Elastic misfit in two-phase polymer. Polymer. 50, 4696–4705. https://doi.org/10.1016/j.polymer.2009.07.037

Molinas, B.J., Lambri, O., Weller, M., 1994. Study of non-linear effects related to the snoek-köster relaxation in Nb. J. Alloys Compd. 211–212, 181–184. https://doi.org/10.1016/0925-8388(94)90477-4

Mori, T., Tanaka, K., 1973. Average stress in matrix and average elastic energy of materials with misfitting inclusions. Acta Metall. 21, 571–574. https://doi.org/10.1016/0001-6160(73)90064-3

Mori, T., Wakashima, K., 1990. Successive Iteration Method in the Evaluation of Average Fields in Elastically Inhomogeneous Materials, in: Weng, G.J., Taya, M., Abé, H. (Eds.), Micromechanics and Inhomogeneity: The Toshio Mura 65th Anniversary Volume. Springer New York, pp. 269–282. https://doi.org/10.1007/978-1-4613-8919-4_18

Mura, T. 1987. Micromechanics of defects in solids. Martinus Nijhoff Publishers, New York.

Nakamura, Y., Yamaguchi, M., Okubo, M., Matsumoto, T., 1992. Effects of particle size on mechanical and impact properties of epoxy resin filled with spherical silica. J. Appl. Polym. Sci. 45, 1281–1289. https://doi.org/10.1002/app.1992.070450716

Ngo, T.D., Kashani, A., Imbalzano, G., Nguyen, K.T.Q., Hui, D., 2018. Additive manufacturing (3D printing): A review of materials, methods, applications and challenges. Compos. Part B Eng. 143, 172–196. https://doi.org/10.1016/j.compositesb.2018.02.012

Pérez-Landazábal, J.I., Lambri, O.A., Bonifacich, F.G., Sánchez-Alarcos, V., Recarte, V., Tarditti, F., 2015. Influence of defects on the irreversible phase transition in Fe–Pd ferromagnetic shape memory alloys. Acta Mater. 86, 110–117. https://doi.org/10.1016/j.actamat.2014.11.054

Pérez-Sáez, R.B., 1998. PhD. Thesis. Universidad del País Vasco.

Pérez-Sáez, R.B., Recarte, V., Nó, M.L., San Juan, J., 1998. Anelastic contributions and transformed volume fraction during thermoelastic martensitic transformations. Phys. Rev. B 57, 5684–5692. https://doi.org/10.1103/PhysRevB.57.5684

Planes, A., Mañosa, L., Acet, M., 2013. Recent Progress and Future Perspectives in Magnetic and Metamagnetic Shape-Memory Heusler Alloys. Mater. Sci. Forum 738–739, 391–399. https://doi.org/10.4028/www.scientific.net/MSF.738-739.391

Planes, A., Mañosa, L., Acet, M., 2009. Magnetocaloric effect and its relation to shape-memory properties in ferromagnetic Heusler alloys. J. Phys. Condens. Matter. 21, 233201.

https://doi.org/10.1088/0953-8984/21/23/233201

Pukanszky, B., VÖRÖS, G., 1993. Mechanism of interfacial interactions in particulate filled composites. Compos. Interf. 1, 411-427. https://doi.org/10.1163/156855493X00266

Reynaud, E., Jouen, T., Gauthier, C., Vigier, G., Varlet, J., 2001. Nanofillers in polymeric matrix: a study on silica reinforced PA6. Polymer. 42, 8759–8768. https://doi.org/10.1016/S0032-3861(01)00446-3

Salas, D., Cesari, E., Golovin, I., Kustov, S., 2012. Magnetomechanical and structural internal friction in Ni-Mn-In-Co metamagnetic shape memory alloy. Solid State Phenom. 184, 372-377. https://doi.org/10.4028/www.scientific.net/SSP.184.372

Schaller, R., Fantozzi, G., Gremaud, G. (Eds.), 2001. Mechanical spectroscopy. Trans Tech Publications, Zurich.

Sharma, V.K., Chattopadhyay, M.K., Shaeb, K.H.B., Chouhan, A., Roy, S.B., 2006. Large magnetoresistance in Ni50Mn34In16 alloy. Appl. Phys. Lett. 89, 222509. https://doi.org/10.1063/1.2399365

Tan, X.P., Tan, Y.J., Chow, C.S.L., Tor, S.B., Yeong, W.Y., 2017. Metallic powder-bed based 3D printing of cellular scaffolds for orthopaedic implants: A state-of-the-art review on manufacturing, topological design, mechanical properties and biocompatibility. Mater. Sci. Eng. C 76, 1328–1343. https://doi.org/10.1016/j.msec.2017.02.094

Van Humbeeck, J., 1985. High damping capacity due to microstructural interfaces, in: Rath, B.B., Misra, M.S. (Eds.), Role of Interfaces on Materials Damping. Proc. ASM's Materials Week and TMS/AIME Fall Meeting, Toronto.

Yan, Q., Dong, H., Su, J., Han, J., Song, B., Wei, Q., Shi, Y., 2018. A Review of 3D Printing Technology for Medical Applications. Engineering 4, 729–742. https://doi.org/10.1016/j.eng.2018.07.021

Yu, S.Y., Liu, Z.H., Liu, G.D., Chen, J.L., Cao, Z.X., Wu, G.H., Zhang, B., Zhang, X.X., 2006. Large magnetoresistance in single-crystalline Ni50 Mn 50-x Inx alloys (x=14-16) upon martensitic transformation. Appl. Phys. Lett. 89, 162503. https://doi.org/10.1063/1.2362581

Zelada-Lambri, G.I., Lambri, O.A., García, J.A., 2006. Mechanical energy losses due to the movement of dislocations in molybdenum at high temperatures (0.3Tm). J. Nucl. Mater. 353, 127–134. https://doi.org/10.1016/j.jnucmat.2006.02.086

Zhao, W., Zhang, F., Leng, J., Liu, Y., 2019. Personalized 4D printing of bioinspired tracheal scaffold concept based on magnetic stimulated shape memory composites. Compos. Sci. Technol. 184, 107866. https://doi.org/10.1016/j.compscitech.2019.107866

Highlights

- Tunable composite polymeric based material
- Mechanically stable functional composite polymeric based material
- Composite material with damping capacity controlled by an external magnetic field
- Eshelby formalism indicates that the composite matrix accommodates all the stresses

Declaration of interests

☒ The authors declare that they have no known competing financial interests or personal relationships that could have appeared to influence the work reported in this paper.

☐The authors declare the following financial interests/personal relationships which may be considered as potential competing interests: